A NEW METHOD OF TIME DOMAIN ANALYSIS FOR STRUCTURE ON A SEMI-INFINITE FOUNDATION

T.-T. Nakagawa (I)
H. Shiojiri (II)
Presenting Author: T.-T. Nakagawa

SUMMARY

This paper presents a new method of time domain analysis for structure-foundation dynamic systems subjected to time-dependent seismic force. The method does not hypothesize the types of elastic waves that may dominate in particular problems. Linear and nonlinear problems are acceptable. Numerical results for linear problems are shown to have a good agreement with those by an existing method in frequency domain analysis.

INTRODUCTION

Accuracy of response analysis of structure on a semi-infinite foundation depends on the treatment of unboundedness of the foundation. A well-known approach is the use of Fourier transform. But this is applicable to only linear problems. The proposed method is a finite element/difference hybrid scheme and uses a direct numerical integration in the time domain. The key is the finite difference part. It computes the radiation of elastic waves into infinity.

PROPOSED SCHEME

We partition the entire domain of structure-foundation system into the following two zones: Zone A which covers the structure and its near-by portion of foundation, and Zone B which covers the remainder portion of foundation. Zones A and B must overlap each other with one mesh width. We call this overlap area the interface boundary, and denote it by Interface I_{AB}. The scheme consists of three computational blocks called the near-field block, the far-field block, and the interface block.

The near-field block computes the response of Zone A by using the usual finite element technique. Thus for elasticity problems, the equation to solve is, in its general form, as follows.

$$[M]\frac{d^2}{dt^2}\{V\} + [C]\frac{d}{dt}\{V\} + [K]\{V\} = \{f\} \qquad (1)$$

where [M], [C], and [K] are the mass matrix, the damping matrix, and the stiffness matrix, respectively, and {V} is the unknown vector of nodal variables (displacements). The right-hand side {f} is the external vector. Here we note that {f} is to contain the unknown variables on Interface I_{AB}. Assuming that {f} at times t and t+k (k: time increment) are known, we integrate (1) using Newmark's β scheme (Ref.1). (The interface block supplies components of {f} on I_{AB}.) For modification to other types of problems

(I) Professor of Mathematics, Konan University, Kobe, Japan
(II) Research Engineer, Central Research Institute of Electric Power Industry, Abiko, Chiba, Japan

such as the dam-reservoir system to be dealt with in Example 3, we combine with (1) the finite element equation representing the governing equation of concern, together with the condition of interaction with the elasticity domain. For example, the governing equation of reservoir water in Example 3 is the wave equation of the potential function, which interacts with the dam surface and with the foundation (reservoir bed) through the continuity of the normal velocity and pressure.

The far-field block computes the response in Zone B. The detail is as follows (Ref.2). We write the equation of elasticity as a first order hyperbolic system using the velocity variables and stress variables, then apply to it a transformation of coordinates that maps the unbounded domain into a rectangle through the integral relation

$$x = \int_0^{x'} \frac{d\xi}{a(\xi)} \quad \text{for } |x'| < \ell_x \quad \text{and } z = \int_0^{z'} \frac{d\zeta}{b(\zeta)} \quad \text{for } -\ell_z < z' \leq 0 \qquad (2)$$

where x and z are the coordinates *before* transformation, and x' and z' are those *after* transformation. Figure 1 shows the zoning of the entire domain after transformation. The denominater a(·) (and b(·) as well) must satisfy that (i) it is unity within Zone A, and (ii) it vanishes when x' approaches $\pm\ell_x$ so that the integral diverges to ± infinity. The resulting equation is

$$\frac{\partial}{\partial t}\begin{bmatrix} u \\ w \\ \sigma_x \\ \tau \\ \sigma_z \end{bmatrix} = a(x')\begin{bmatrix} 0 & 0 & 1/\rho & 0 & 0 \\ 0 & 0 & 0 & 1/\rho & 0 \\ \lambda+2\mu & 0 & 0 & 0 & 0 \\ 0 & \mu & 0 & 0 & 0 \\ \lambda & 0 & 0 & 0 & 0 \end{bmatrix} \frac{\partial}{\partial x'}\begin{bmatrix} u \\ w \\ \sigma_x \\ \tau \\ \sigma_z \end{bmatrix} + b(z')\begin{bmatrix} 0 & 0 & 0 & 1/\rho & 0 \\ 0 & 0 & 0 & 0 & 1/\rho \\ 0 & \lambda & 0 & 0 & 0 \\ \mu & 0 & 0 & 0 & 0 \\ 0 & \lambda+2\mu & 0 & 0 & 0 \end{bmatrix} \frac{\partial}{\partial z'}\begin{bmatrix} u \\ w \\ \sigma_x \\ \tau \\ \sigma_z \end{bmatrix} \qquad (3)$$

where ρ is the mass density, λ and μ are the Lamé coefficients, u and w are the velocity variables, and σ_x, τ, and σ_z are the stress variables. (If ρ, λ, and μ depend on (x,z), then they have to be expressed in terms of (x',z').) We solve this equation by Lax-Wendroff differencing technique (Ref.3), which has been developed for computation of shocks in gas dynamics problems. Assuming that the values of the unknown variables are given at time t in Zone B and on Interface I_{AB}, we can obtain those at time t+k inside Zone B. For the dam-reservoir system , we solve simultaneously the wave equation which is written in the form of hyperbolic first order system for the pressure and two velocity variables.

The interface block relates the variables of the above two blocks across I_{AB} at each time step. In our computer program, we employ quadrilateral linear elements for Zone A. Thus, the task of this block is as follows.

(I) From Zone B to Zone A: Numerical line integration of stress variables to yield the equivalent nodal forces.

(II) From Zone A to Zone B: Numerical differentiation of the nodal displacement variables to yield the stress components.

Figure 2 shows the entire scheme. In the scheme, the above three blocks are invoked successively within each time step.

EXAMPLES

Example 1. Semi-infinite foundation without structure.

We solved this problem when the foundation undergoes a harmonic uniform loading. Figure 3 gives the equivalent stiffness for vertical loading. This value is obtained from those computed results in which the transient response has decayed out from the near-field portion of foundation. (The same principle will be applied to Examples 2 and 3 also to obtain the frequency response.) For comparison we put in Fig. 3 the theoretical value by the method of Fourier transfrom (Ref.4), together with the one by the finite element method with transmitting boundary in the frequency domain (Ref.5). (In the following, we shall call the latter method the transmitting boundary method. We put a viscous boundary beneath the finite element model of foundation to absorb the vertically scattering wave components when we use this method.) The results by these three methods show a good agreement.

Example 2. Effect of embedment of a structure.

We solved three cases of embedment, as shown in Fig. 4, when the structure undergoes the vertically propagating sinusoidal S-wave. Figure 5 gives the magnification factor of acceleration at the top of structure. Figure 6 shows a transient profile of the acceleration field in our extreme cases of embedment, i.e., Cases I and III, when the acceleration reaches its maximum at the top of structure. Apparently the acceleration induced in the structure decreases considerably as the depth of embedment increases. We remark that when a slip boundary characterized by Fig. 7 is assumed between the basement and the foundation, the acceleration and stresses induced in the structure are reduced further.

Example 3. Gravity dam.

Figure 8 shows the geometry of a gravity dam. We solved this problem under empty and full reservoir water conditions. Figure 9 is a profile of acceleration field of dam in the case of full reservoir water due to the vertically propagating sinusoidal S-wave, and Fig. 10 gives the distribution of hydrodynamic pressure on the dam surface. The results appear reasonable. According to our preliminary computation in the limiting case of rigid dam on a rigid foundation (reservoir bed), the pressure distribution on the dam surface agrees well with the well-knwon Westergaard formula (Ref.6) within 5% error, if the excitation frequency is low, typically in the range of below 3 Hz for our geometry. Figure 11 shows the time history of acceleration at the top of dam under the full reservoir water condition. Figures 12 and 13 give the magnification factor of acceleration at the top of dam under empty and full reservoir conditions. We again compare our results with those by the transmitting boundary method. The agreement between the two is good.

CONCLUSION

We have developed a method of time domain analysis for structure/foundation dynamical systems. The radiation of elastic waves is dealt with through the use of the coordinate transformation and the finite differencing technique for shock computation.

For linear problems, we have shown that the results agree well with those by the transmitting boundary method. Because of the construction of our algorithm, the extension to nonlinear problmes is straightforward as mentioned in Example 2. Further, we remark that irregular foundation problems and the quasi three-dimensional problems as well are simply variants of what have been presented here.

We do not anticipate theoretical difficulties in the extension to truly three-dimensional analysis. We are investigating the problem of accracy and efficient use of computing resources for this extension.

REFERENCES

1. N.M. Newmark, "A method of computation for structural dynamics," Proc. ASCE, vol. 85, No. EM3, 67 - 94 (1959).

2. T.-T. Nakagawa, "Numerical solution in the near field to linear hyperbolic systems, with application to an elastic foundation problem," Computing Methods in Applied Sciences and Engineering V, (R. Glowinski and J.L. Lions, eds.), North-Holland Publishing Co., 1982.

3. G. Strang, "On the construction and comparison of difference schemes," SIAM J. Numerical Analysis, vol. 5, 506 - 517 (1968).

4. K. Hanada, "Analysis on dynamic behaviours of soil-structure systems; (1) Dynamic response of a semi-infinite elastic body with plane strain by excitation on its surface," Res. Rep. 74013, Central Research Institute of Electric Power Industry, Japan, 1975 (in Japanese).

5. A. Gomez-Masso et al., "Soil-structure interaction in different seismic environments," Report No. UCB/EERC-79/18, EERC, University of California, August 1979.

6. H.M. Westergaard, "Water pressures on dams during earthquakes," Trans. ASCE, vol. 98, 418 - 433 (1933).

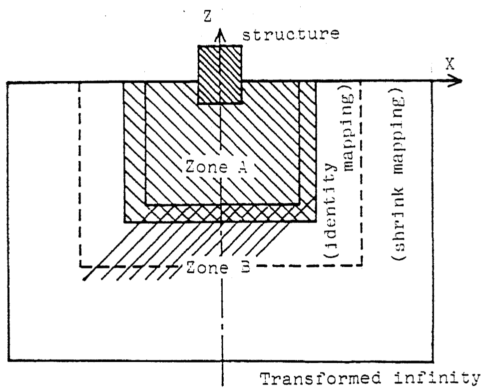

Fig. 1 Zoning for the structure-foundation interaction problem (after coordinate transformation)

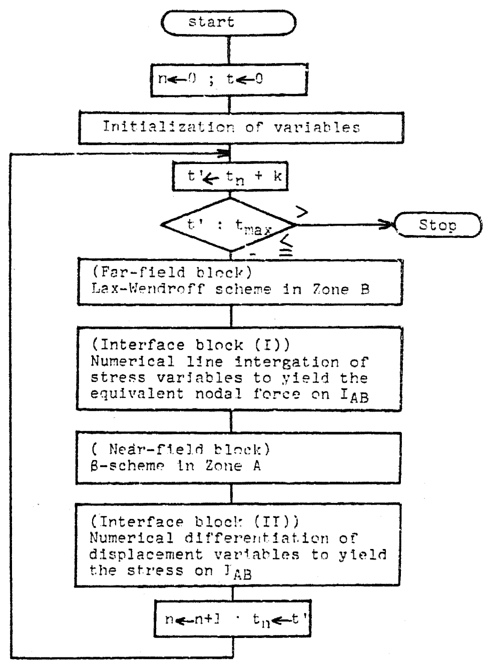

Fig. 2 Flow diagram of the proposed scheme

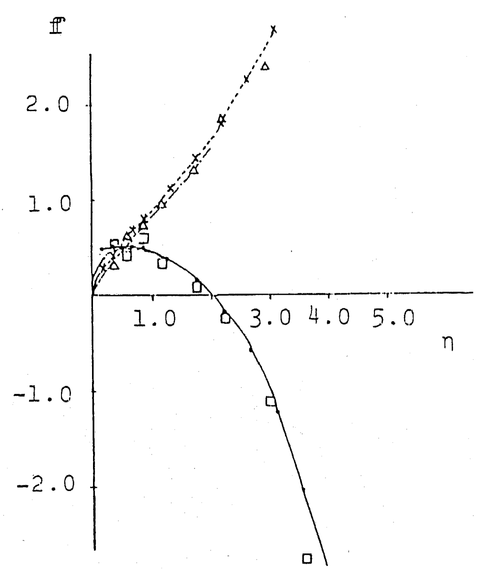

□ Ref — Proposed method
△ Imf — Proposed method

—•—•— Ref — Transmitting boundary method
-x--x- Imf — Transmitting boundary method

-·—·- Analytical solution

$f = p/(\pi\mu x)$

$\eta = \omega d/Vs$

P : complex amplitude of external force

x : Complex amplitude of vertical displacement at the midplacement

d : width of uniform loading

Vs: velocity of S wave

Fig. 3 Equivalent stiffness of semi-infinite foundation due to uniform vertical loading

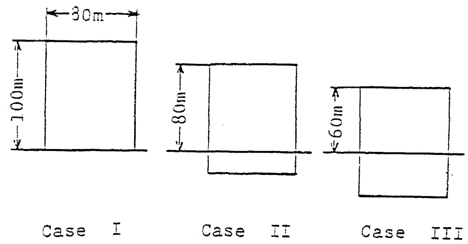

Material properties

	ρ (t/m^3)	λ (t/m^2)	μ (t/m^2)
structure	0.12	4.2×10^5	6.3×10^5
foundation	0.24	8.3×10^4	1.25×10^5

Fig. 4 Three cases of embedment of a structure

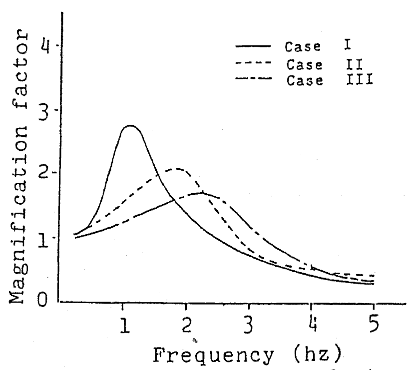

Fig. 5 Magnification factor of the horizontal acceleration at the top of structure due to the vertically propagating sinusoidal S wave

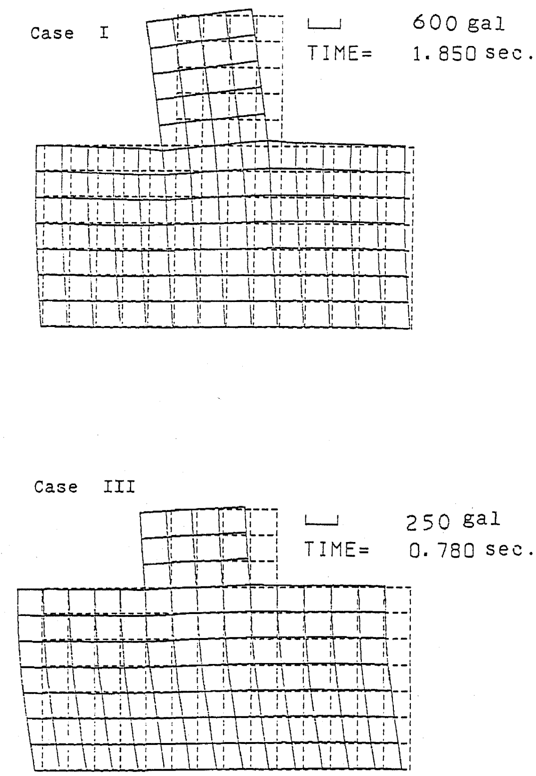

Fig. 6 Transient profile of acceleration field of structure and foundation

Amp. = 200 gal

Freq.= 1 Hz

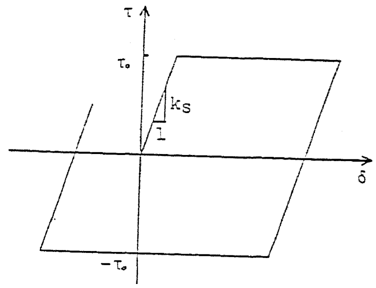

Fig. 7 Shear stress vs. relative displacement relationship on the slip boundary

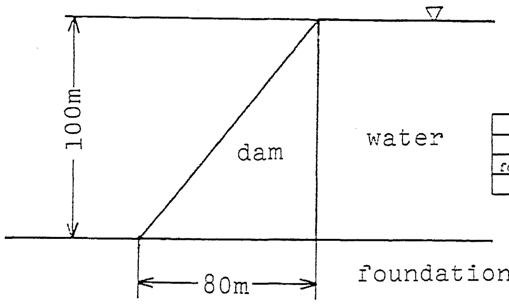

Matrial properties

	$\rho(t/m^3)$	$\lambda(t/m^2)$	$\mu(t/m^2)$	$k(t/m^2)$
dam	0.24	2.4×10^6	3.5×10^6	4.3×10^6
foundation	0.24	8.3×10^5	1.25×10^6	1.57×10^6
water	0.1	-	-	2.1×10^5

Fig. 8 Geometry of a gravity dam

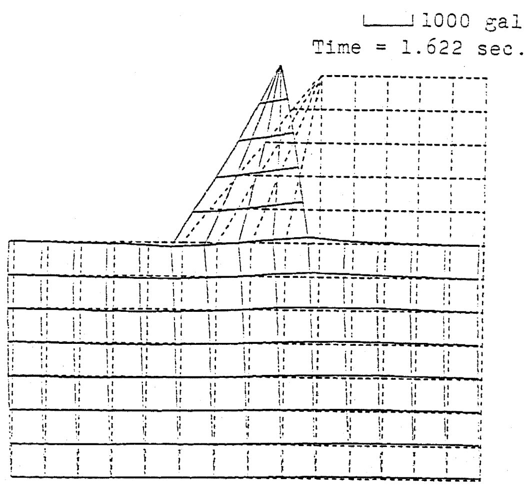

Acceleration of S wave Amp.=200 gal
Freq.= 3 Hz

Fig. 9 Transient profile of acceleration field of gravity dam and foundation due to the vertically propagating sinusoidal S wave

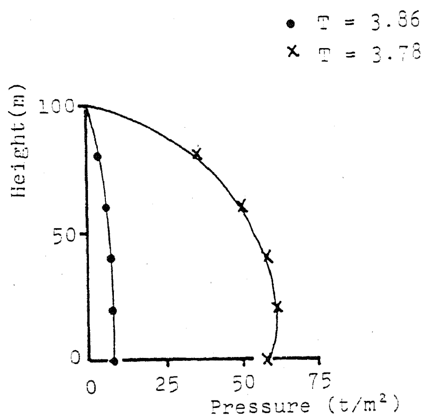

Fig.10 Hydrodynamic pressure on the dam surface

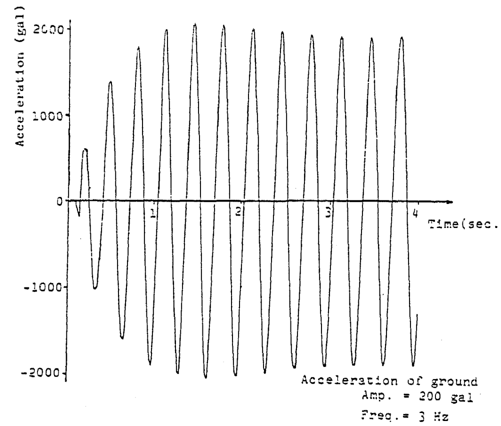

Fig.11 Time histroy of the horizontal acceleration component at the top of dam

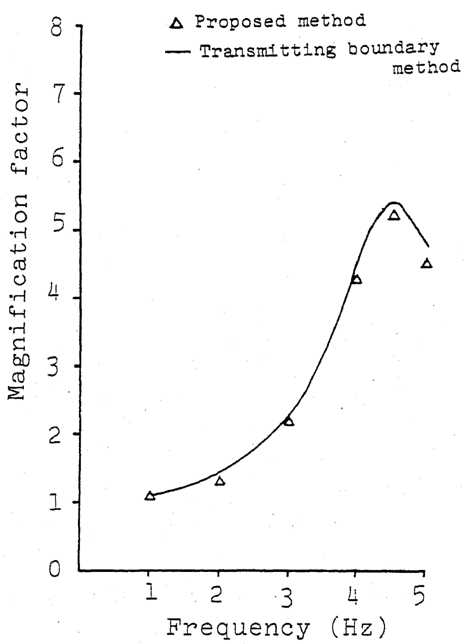

Fig.12 Magnification factor of the horizontal acceleration at the top of dam with empty reservoir water

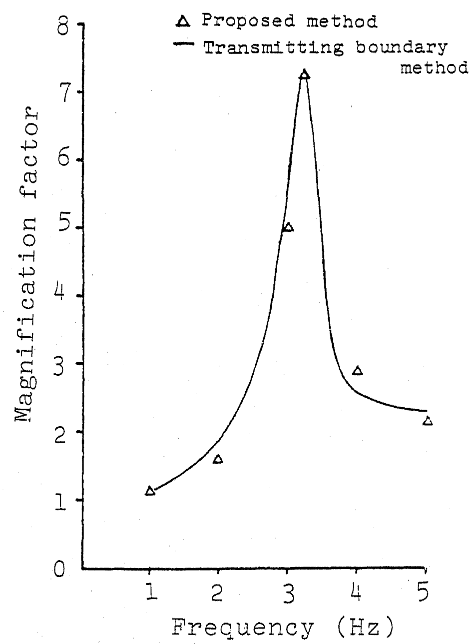

Fig.13 Magnification factor of acceleration at the top of dam with full reservoir water